

Original Article

Enhancing Dyslexia Detection and Classification based on Wavelet Scattered Transform and Dirichlet Mixture Model

J. Jincy^{1,2}, P. Subha Hency Jose¹, P. Sweety Jose³, S.Thomas George¹, Mary Vasanthi Soosaimariyan⁴, Sujin Jose Arul⁵

¹Department of Biomedical Engineering, Karunya Institute of Technology and Sciences, Coimbatore, Tamilnadu, India.

²Department of Electronics and Communication Engineering, CSI College of Engineering, Ketti, Tamilnadu, India.

³Department of Electrical and Electronics Engineering, PSG College of Technology, Coimbatore, Tamilnadu, India.

⁴Department of Electronics and Communication Engineering, St Xavier's Catholic College of Engineering, Nagercoil, Tamilnadu, India.

⁵Department of Mechanical Engineering, New Horizon College of Engineering, Bangalore, India.

⁵Corresponding Author : sujinjooseer@gmail.com

Received: 21 March 2025

Revised: 20 May 2025

Accepted: 29 May 2025

Published: 28 June 2025

Abstract - Since traditional diagnosis methods rely on behavioural testing rather than biological signs, detecting dyslexia is complicated. Information Extraction about the brain actions participated in various jobs, and delving into their biological underpinnings is challenging. As a result, using biomarkers can aid in both the diagnosis and a deeper comprehension of particular learning problems, including dyslexia. Differences between controls and dyslexic subjects can be found using Electroencephalography (EEG) signals with the proper signal processing and artificial intelligence approaches. In this work, we have combined the benefits of the Dirichlet Mixture Model (DMM) and wavelet scattered transform (WST) to convert the EEG data into high-level representations that enable the detection of dyslexic discriminative descriptors. Furthermore, we have developed a predictive Stoer-Wagner algorithm-based Naïve Bayes (SW-NB) classifier that performs exceptionally well with an exploratory examination of the EEG signals to detect dyslexia accurately. The suggested SW-NB classification model, in conjunction with WS-DMM, may significantly increase the accuracy of disease identification. A dataset of confused students' brainwaves is used to test the suggested classification model, and the findings are more promising.

Keywords - EEG signal, Dyslexia detection, Wavelet scattered dirichlet mixture model, Signal denoising, Naïve bayes classifier.

1. Introduction

One of the well-known non-invasive methods used to learn about brain activity is Electroencephalography (EEG) [1]. It has been used extensively for a variety of purposes, including the investigation of brain processes included in neurological diseases like Parkinsonian syndromes [2, 3], Alzheimer's disease [4, 5], epileptic disorders [6-8], and other psychiatric disorders like schizophrenia [9]. Furthermore, experimental neuropsychology has extensively used EEG to learn more about the parts of the cortex involved in processing various stimuli. This is the situation with learning disabilities, whose neurological causes are still unidentified. Additionally, clarifying the brain mechanisms behind language processing provides a direction to diagnose these diseases on time. One of the most common specific developmental learning disorders, dyslexia, is defined as a specific reading acquisition deficit that low IQ, inadequate educational opportunities, or evident sensory or neurological impairment cannot explain. It

is estimated that 5–15% of students have dyslexia [7]. It is recognized as a neurological condition affecting word recognition in children and students, leading to writing and text comprehension challenges. Social isolation, frustration, and self-esteem issues are further consequences of dyslexia. For both individuals and society at large, dyslexia is a severe problem. It is among the most prevalent learning disabilities, impacting a considerable segment of the populace [8]. Numerous academic disciplines, including linguistics, psychology, pedagogy, medicine, and the social sciences, assess dyslexia [9]. The molecular and neurological foundations, language processes, cognitive and behavioral components, educational consequences, and social and cultural variables are some of the features of dyslexia that are examined in each field. These multidisciplinary methods offer a thorough comprehension of dyslexia and guide the creation of efficient support systems and therapies [10]. Various predispositions, some inherited from family lines and others



impacted by early life events, significantly contribute to dyslexia. When used in the early stages, prevention programs and customized intervention tasks may help to minimize behavioural problems in dyslexic youngsters. Early detection and intervention of dyslexia depend on understanding its risk factors, which comprise low birth weight, early birth, and family antiquity of the disorder [11]. It is critical to acknowledge that dyslexia is a chronic disorder that can be managed, and its effects on a person's life can be lessened, even if it persists into adulthood. However, since most behavioural tests created for this purpose involve reading or writing assignments, early diagnosis is now a complex process [12].

Most of the time, behavioural tests that gauge reading and writing proficiency are used to diagnose dyslexia. Consistent reading and language tests, interpretations, and teacher reports are commonly used with other measures to identify children who have dyslexia [13]. These tests measure a child's understanding, fluency, and accuracy in reading. Exogenous variations, such as children's motivation or mood, frequently impact the tests, leading to basic mistakes in the diagnosis [14]. Concerns regarding dyslexia may arise if a youngster continuously performs worse in reading than their peers despite receiving proper training [15]. A definitive diagnosis, however, may require further neuropsychological or medical testing, and the precise standards and timeline for identification may differ [16, 17].

In order to get over these obstacles, Machine Learning (ML) techniques have been utilized to spontaneously analyse EEG information and spot patterns that may point to dyslexia. It may be possible to identify dyslexia at an earlier age by combining EEG and machine learning approaches, providing people with the tools they need to succeed [18, 19]. In this research, we have combined the benefits of the Dirichlet Mixture Model (DMM) and Wavelet Scattering Transform (WST) to develop helpful signal illustrations from EEG data that enable the detection of dyslexic discriminatory characteristics. A subset of the data is governed by a collection of wavelets in our model, which we call the Wavelet Scattered Dirichlet Mixture Model (WS-DMM). A predictive Stoer-Wagner algorithm-based Naïve Bayes (SW-NB) classifier that performs exceptionally well with an exploratory examination of the EEG signals was developed because we recognize the significance of accurate dyslexia identification.

This paper's reminder is arranged as follows: Section 2 outlines a few recent research introduced in the application of early diagnosis of dyslexia, and Section 3 explains the suggested model's step-by-step algorithmic architecture. Along with a performance comparison with a few previous efforts, Section 4 gives the experimental endorsement and findings of the anticipated study. Section 5 provides a summary and rationale for the proposed work's conclusion. Existing approaches typically apply shallow classifiers such

as SVMs or basic neural networks on linear features. However, these often fail to represent the complex non-linear EEG characteristics associated with dyslexia. This research introduces a novel hybrid model combining WS-DMM for enhanced feature extraction and a graph-theory-based Stoer-Wagner Naïve Bayes classifier, significantly improving classification performance over prior work.

2. Literature Survey

Pyrolysis Some recent works implemented to detect dyslexia in an early stage are highlighted in this section as follows:-

The complex brain processes linked to dyslexia were investigated using cross-frequency coupling on EEG signals from 48 Spanish readers aged seven who were part of the LEEDUCA study. In order to capture the collaboration among several frequency bands through low-level auditory processing inputs, the study relies on Cross-Frequency phase Synchronization (CFS) maps. Gaussian Mixture Models are then used to quantify and categorize CFS activations, providing a condensed depiction of EEG activation maps.

While Parmar et al. [20] used WST for primitive-stage detection, our approach further enhances it using a Dirichlet mixture-based representation to capture non-linear feature distributions: spectral data attributes, connectivity attributes with autoencoders, and mixture attributes. The two datasets were selected for many motives, comprising the statistic that they came from separate nations and were gathered during distinct tasks. Another important consideration was that the participants' ages ranged from 7 to 12 years old when their educational journeys began.

GuhanSeshadri et al. [21] suggested a deep and shallow neural network (DNN) based framework for the early identification and categorization of Learning Disabilities (LD) in children without LD based on rest EEG signals. Twenty youngsters (ages 8–16) with LD and twenty without LD participated in the study. The raw EEG signal is pre-processed using the Digital Wavelet Transform (DWT), and different features are fetched from alpha, delta, beta, and theta bands. The most pertinent features were chosen using a filter-based feature selection method, which lessens the computational load on models. In order to examine the performance, these sorted cumulative characteristics were then assessed independently by neural network and ML classifiers (deep and shallow) models.

Nicolás J. Gallego-Molina et al. [22] suggested a novel method that combines the creation of a deep learning paradigm with two stages for identifying developmental dyslexia with the conversion of EEG signals into image frames while taking into account the dynamics of CFS, which are participated in low-level auditory dispensation. With a balanced accuracy of up to 83%, the deep learning technique

uses temporal and spatial statistics with the image frames to identify discriminatory outlines of phase synchronization across time. Zbigniew Gomolka et al. [23] suggested using a student's cell phone to capture the spatiotemporal attentional trajectory, which a DNN Long Short-Term Memory (LSTM) would subsequently analyse. There were 145 participants in the study, 69 boys and 66 girls; all were 9 years old. Sessions of observation that were recorded were packets encapsulating the child's spatiotemporal attention trajectories created during task execution, which made up the neural network's input signal. Few models address the complexity and variability of EEG signals in dyslexic individuals. Our proposed WS-DMM captures translation-invariant features while Stoer-Wagner's optimization enhances the classification of graph-like dependencies within EEG channels, closing this gap.

3. Results and Discussion

The linear relationship between a response variable and covariates facilitates parameter estimation and result interpretation in regression and classification models. However, the suitability of these assumptions determines how well such a model performs [24]. Therefore, we include the Dirichlet mixture model of simple distributions to model the EEG data in our proposed WS-DMM model, which is more adaptable in capturing nonlinear correlations. The translation invariant, stable, and more informative signal representations needed for efficient classification are then fetched from the simulated distribution by applying WST. The input EEG signal must also be pre-processed before modelling to get meaningful performance. The components of the suggested dyslexia detection model are exhibited in Figure 1.

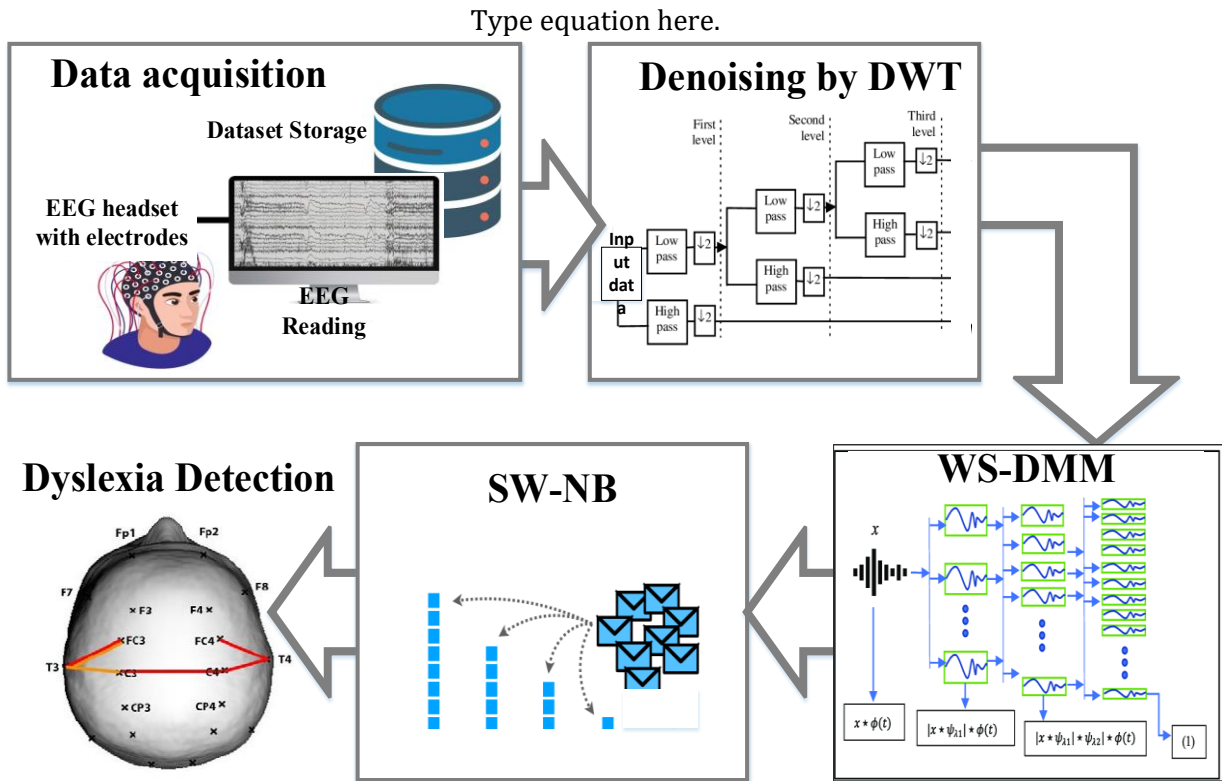


Fig. 1 Building blocks of the anticipated dyslexia detection model

3.1. Mathematical Modelling of Input Data

The original input EEG signal dataset is represented as:

$$I_{EEG} = \{I_1, I_2, \dots, I_n\} = \sum_{i=1}^n I_i \quad (1)$$

Where, I_i - input EEG signal of the i^{th} subject involved in the experiment and n the number of subjects involved in the investigation.

3.2. Wavelet Denoising

Artifact noises, such as eye scrolling noise, eye flashing noise, Electromyogram (EMG) noise, muscle movement noise

and interference from electrical equipment indications, can taint the original EEG signal I_{EEG} while it is being recorded.

Thus, DWT has been suggested as a signal-denoising technique. Because DWT assumes that the objects will have substantial amplitudes in the appropriate frequency crowds (bands), it breaks down the EEG signal into many bands.

Typically, the three primary phases build the DWT denoising process: (i) signal decomposition, (ii) Thresholding, and (iii) signal reconstruction. Figure 2 shows the DWT structure with decomposition level $d = 2$.

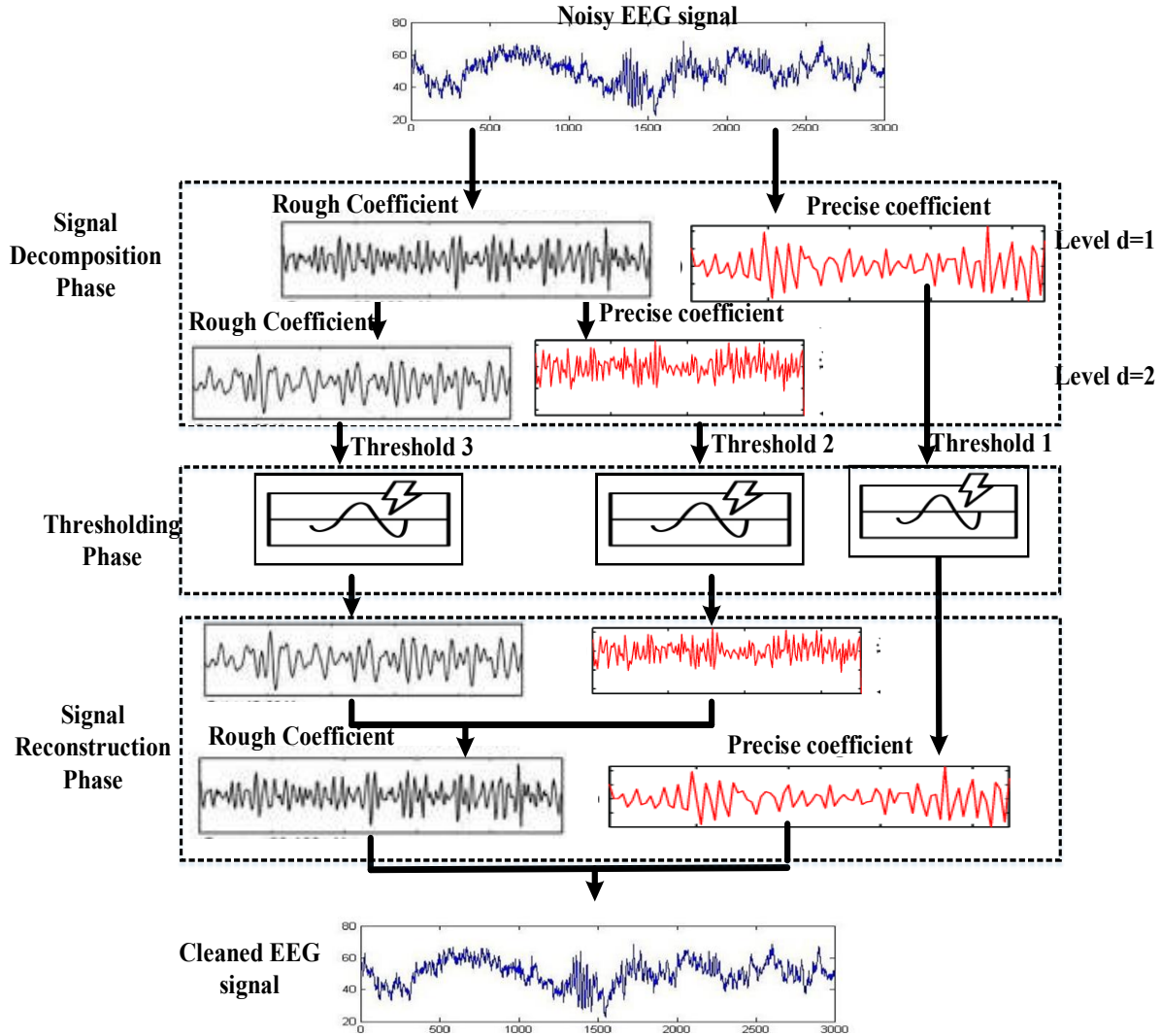


Fig. 2 Wavelet denoising procedure with decomposition level d=2

The raw input EEG signals with n samples $I_{EEG}(t) = \{I_1, I_2, \dots, I_n\}$ is splitted into two tiers, and each tier will be decomposed into two components, namely, rough coefficients C^{rough} and precise coefficients $C^{precise}$. $C^{precise}$ is executed using a high-pass filter, though C^{rough} will further decomposed for the next tier. The approximation and detail coefficients can be estimated as:

$$C_i^{rough}(t) = \sum_{u=-\infty}^{\infty} C_{i-1}^{rough}(u) \Phi_i(t-u) \quad (2)$$

$$C_i^{precise}(t) = \sum_{u=-\infty}^{\infty} C_{i-1}^{precise}(u) \Psi_i(t-u) \quad (3)$$

Where $C_i^{rough}(t)$ and $C_i^{precise}(t)$ represents the rough and precise coefficients of level i and Φ, Ψ are the scaling and shifting parameters, respectively. The thresholding value is ideally set for each level as per the standard deviation (σ) of noise amplitude, which can be mathematically written as:

$$I_{EEG}^{noisy}(n) = I_{(n)} + \sigma N_{(n)} \quad (4)$$

Where $I_{(n)}$ represents the raw EEG signal, N represents the noise, σ represents the amplitude of the noise and n represents the sample numbers.

The denoised EEG indication is then recreated by performing iDWT using the below Equation. (5).

$$I_{EEG}^{clean} = \sum_{u=-\infty}^{\infty} C_d^{rough}(u) \Phi_i(t-u) + \sum_{i=1}^d \sum_{u=-\infty}^{\infty} C_{i+1}^{precise}(u) \Psi_i(t-u) \quad (5)$$

3.3. Wavelet Scattered Dirichlet Mixture Model (WS-DMM)

The denoised EEG signal I_{EEG}^{clean} is modelled using DMM as a boundary of finite mixing model. The distribution I_{EEG}^{clean} can be modelled as a mixture of simple distributions, with probability or density function as follows:

$$P(I_{EEG}) = \sum_{y=1}^Y p_y F(I_{EEG}, \phi_y) \quad (6)$$

Where p_y is the mixing proportion, and $F(I_{EEG}, \phi_y)$ is the probability or density I_{EEG} under a distribution $F(\phi)$. Our initial assumption is that the number of mixing elements Y is finite. In this condition, a typical prior for p_y is a symmetric Dirichlet distribution, with density function defined as:

$$P(p_1, 2, \dots, p_y) = \frac{\Gamma(Y)}{\Gamma(Y)^Y} \prod_{y=1}^Y p_y^{(Y-1)} \quad (7)$$

Where $p_y \geq 0$ and $\sum p_y = 1$.

A WST that repeatedly uses nonlinear modulus, conventional wavelet transform, and mean operators [25]. For ease of handling, let $I(t)$ is the Dirichlet modelled signal, which is further used for the analysis. The LPF (low-pass filter) Γ and wavelet function (λ) are designated to generate filters that encompass all the confined frequencies. Let $\Gamma_j(t)$ - LPF that provides locally conversion invariant details I at a predetermined scale τ . The wavelet directories are represented as Δ_g having octave frequency resolution Q_g . The multiscale high-pass filter banks $\{\lambda_{j_g}\}_{j_g \in \Delta_g}$ can be fabricated by stretching the wavelet λ .

The convolution $C_0 I(t) = I * \Gamma_j(t)$ produces an invariant property of local translation I but also causes high-frequency data loss. A wavelet modulus transform can be utilized to recover the lost high frequencies.

$$|W_1| I = \{C_0 I(t), I * \Gamma_{j_1}(t)\}_{j_1 \in \Delta_t} \quad (8)$$

The wavelet modulus coefficients are averaged to determine the first-order scattering coefficients with Γ_j :

$$C_1 I(t) = \{|I * \lambda_{j_i} * \Gamma_j(t)\}_{j_i \in \Delta_t} \quad (9)$$

To retrieve the missing data lost due to averaging, noting that $C_1 I(t)$ it is regarded as the low-frequency element of $|I * \lambda_{j_1}|$ complementary high-frequency coefficients can be fetched by:

$$|W_2| |I * \lambda_{j_i}| = \{C_1 I(t), |I * \lambda_{j_i}| * \Gamma_{j_2}(t)\}_{j_2 \in \Delta_2} \quad (10)$$

The second-order scattering coefficients are further defined as:

$$C_2 I(t) = \{|I * \lambda_{j_i} * \lambda_{j_2} * \Gamma_j(t)\}_{j_i \in \Delta_t}, i = 1, 2 \quad (11)$$

Repeating the above steps describes wavelet modulus convolution

$$H_m I(t) = \{||I * \lambda_{j_i} * \dots * \lambda_{j_m}\}_{j_i \in \Delta_t}, i = 1, 2, \dots, m \quad (12)$$

Averaging $H_m I(t)$ with Γ_j gives the m^{th} -order scattering coefficients

$$C_m I(t) = \{||I * \lambda_{j_i} * \dots * \lambda_{j_m} * \Gamma_j(t)\}_{j_i \in \Delta_t}, i = 1, 2, \dots, m \quad (13)$$

Now, the absolute scattering matrix is obtained as:

$$CI(t) = \{C_m I(t)\}_{0 \leq m \leq r} \quad (14)$$

Where r is the maximum order of decomposition. The scattering matrix obtained in Equation (14) describes the characteristics of the input signal by combining scattering coefficients of all orders.

3.4. Dyslexia Detection by SW-NB

This study uses the advantages of Naïve Bayes (NB) classifiers to identify dyslexia. These classifiers perform well with relatively small datasets, avoid dimensionality-related issues, and do not suffer from overfitting. NB classifiers divide data into distinct classes using a series of algorithms that all adhere to the same concept known as the Bayes Theorem. On the other hand, NB works effectively when the predictors are assumed to be independent and functionally independent. When NB performs between these two assumptions, its performance is inferior. An ensemble that combines multiple classifiers may be able to fix this issue. For that purpose, in this paper, we have integrated the advantages of the Stoer-Wagner algorithm with the NB classifier to produce a better predictive performance. Let the scattering coefficients $\{C_1, C_2, \dots, C_m\}$ be used as the features for classification, which A is the output label. The relationship between the given class variable A and dependent feature vector C_m can be written as:

$$P(A|C_1, \dots, C_m) = \frac{P(A)P(C_1, \dots, C_m|A)}{P(C_1, \dots, C_m)} \quad (15)$$

Since $P(C_1, \dots, C_m)$ is perpetual given the input, the below classification rule may be applied:

$$P(A|C_1, \dots, C_m) \propto \frac{P(A) \prod_{i=1}^m P(C_i|A)}{P(C_1, \dots, C_m)} \quad (16)$$

$$\hat{A} = \arg \max_A P(A) \prod_{i=1}^m P(C_i|A) \quad (17)$$

Algorithm 1: SW-NB classifier

Input: Scattering coefficients C_m

Output: Labelled outputs \hat{A}

Let Out=INF

For ($i = 0, i < m - 1, i + +$)

Calculate *min C ut* value as

$$\text{min C ut} = \min(\text{min C ut}, C_i)$$

If (*min C ut* < Out)

Out = *min C ut*

```

 $\hat{A}=1$ 
Else
 $\hat{A}=0$ 
End if
Return  $\hat{A}$ 

```

The independent features in the proposed SW-NB classifier are directly classified to the output label using the above classification rules in Equation (14) and (15), if a connected component exists, the decision rule can be altered according to the Stoer-Wagner Algorithm. The algorithmic procedure of the proposed SW-NB classifier is precised in algorithm 1.

4. Results & Performance Comparison

Section 4 contains the investigational findings, the performance analysis of the suggested model, and a thorough description of the dataset used to validate it. Furthermore, to demonstrate the supremacy of the suggested model, its enactment is contrasted with a few known classifiers.

4.1. Dataset Used

In this paper, we have used an online available dataset called confused student EEG brainwave data, which is freely fetched using the link <https://www.kaggle.com/datasets/wanghaohan/confused-ee>. Ten college students' EEG signals were recorded as they watched MOOC video snippets, and the results are included in this dataset-twenty movies, ten in each category, covering subjects like stem cell research and quantum mechanics. Each video was roughly two minutes long. The pupils wore a single-channel cordless mindset that assessed activity across the frontal lobe. The Mind Set detects the voltage between two electrodes, one ground and one reference, that are in contact with each ear and an electrode placed on the forehead. On a scale of 1 to 7, with 7 representing the most puzzling, the student assessed his or her level of confusion at the end of each session.

4.2. Performance Analysis

The mathematical modelling of the enactment factors such as Sensitivity, Accuracy and Specificity used for evaluation is as follows:

$$Accuracy = \frac{P_{True}N_{True}}{P_{True}N_{True} + P_{False}N_{False}} \tag{18}$$

$$Sensitivity = \frac{P_{True}}{P_{True} + N_{False}} \tag{19}$$

$$Specificity = \frac{N_{True}}{N_{True} + P_{False}} \tag{20}$$

Where, P_{True} are the correctly classified positives, N_{True} are the correctly classified negatives, P_{False} are the misclassified positives and N_{False} are the misclassified negatives.

4.3. Performance Comparison

To validate the enactment of the anticipated dyslexia detection model, in this research, we have used the students' responses in the experiment in two circumstances, namely audio recognition and visual discrimination. This research mainly uses the SW-NB classifier for EEG signal classification. As shown in Table 1, many brain ROIs are developed to pinpoint distinct dyslexia patterns across various brain areas. This aids in locating brain regions with more noticeable EEG activation patterns.

Figure 3 shows the performance values of the proposed SW-NB classifier model with the first experimental condition, in which words were recognized by sound. The performance values of the suggested SW-NB classifier model under the second experimental condition, in which participants were required to distinguish word groups with phonologically similar characteristics visually, are displayed in Figure 4. In order to prove the significance and the superiority of the anticipated classification model, the enactment of the anticipated classification model is compared against multiple classifiers proposed in [26-28] for the two above-mentioned experimental conditions (audio recognition and visual discrimination). Our proposed classification model, SW-NB, is an integrated version of the traditional NB classifier. We have also compared the enactment of the anticipated SW-NB classification model with the traditional NB classifier to show the necessity of the anticipated new classification model.

Table 1. Brain RoI segments and their corresponding channels

Area	Channels
Brain (Entire)	F3, AF3, FC5, P7, P7, AF4, O1, FC6, F4, T8, P8 and O2
Hemisphere (Left)	F3, AF3, FC5, P7, T7, O1
Hemisphere (Right)	F4, AF4, T8, FC6, P8, O2
Frontal (Left)	F3, AF3
Temporal (Left)	FC5, T7
Occipital (Left)	P7, O1
Frontal (Right)	F4, AF4
Temporal (Right)	FC6, T8
Occipital (Right)	P8, O2

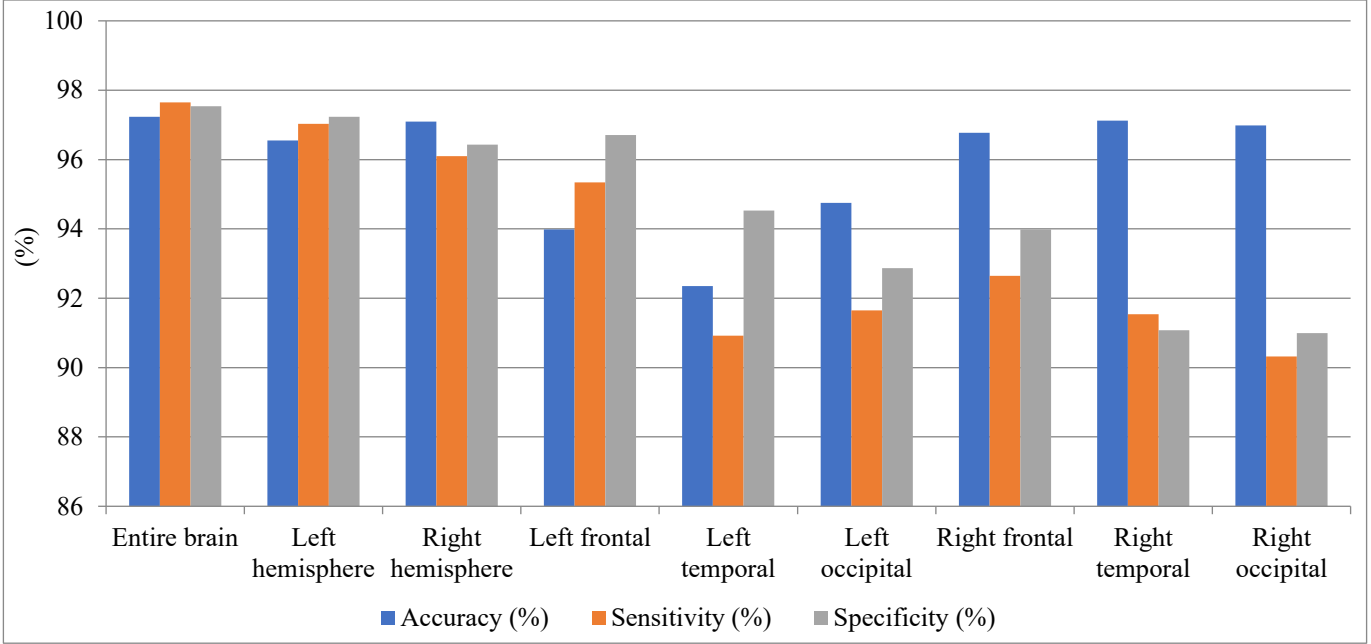


Fig. 3 Performance of the anticipated SW-NB classifier model with the first experimental condition

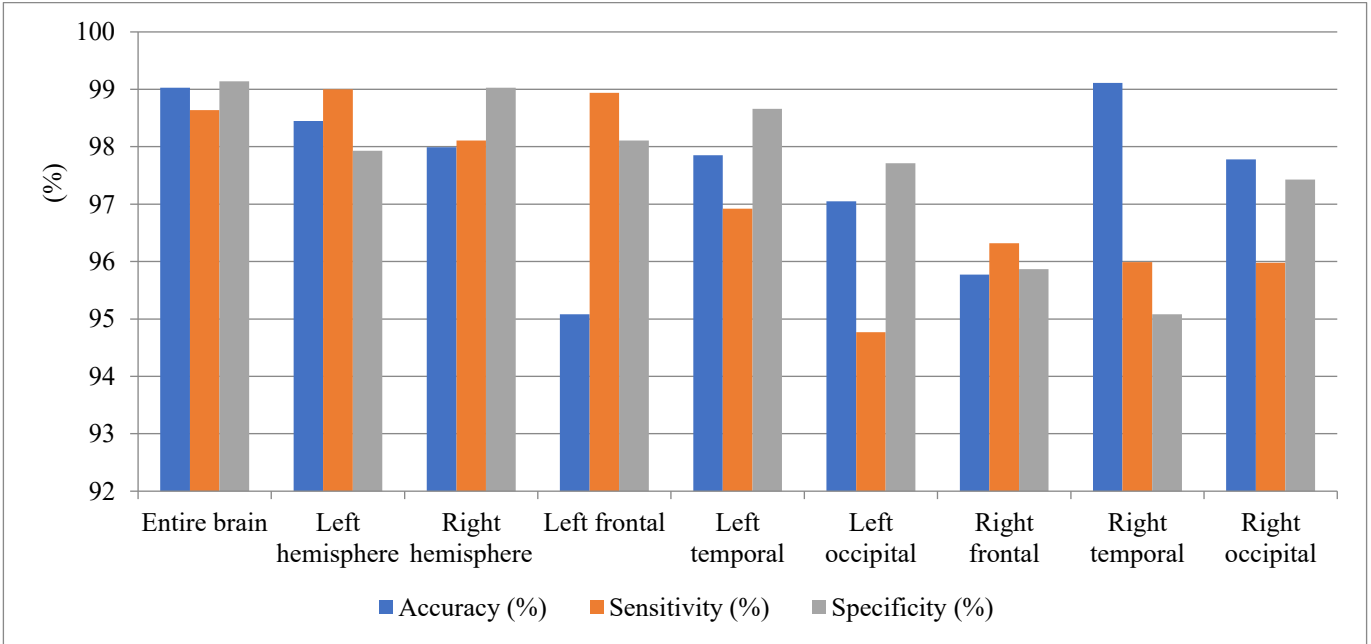


Fig. 4 Performance of the anticipated SW-NB classifier model with the second experimental condition

Table 2 displays the accuracy comparison of several classification models for both experimental conditions.

Table 3 displays the performance analysis of several classification models regarding sensitivity for both experimental conditions.

Table 4 compares the performance of several classification models for both experimental conditions in terms of specificity.

From Tables 4 to 6, it is perceived that the anticipated SW-NB classification model overtakes all the other classification models in terms of sensitivity, accuracy and specificity in both experimental conditions.

The proposed SW-NB classification model attains a maximum accuracy of 99.11% for right temporal RoI, maximum sensitivity of 99% for left hemisphere RoI and maximum specificity of 99.14% for entire brain RoI during the second experimental condition.

Table 2. Accuracy comparison of several classification models

Area	First Experimental Condition				Second Experimental Condition			
	SW-NB	NB	SVM	RF	SW-NB	NB	SVM	RF
Entire brain	97.23	96.88	59.38	96.24	99.03	98.78	78.13	98.01
Left hemisphere	96.55	96.54	65.63	93.032	98.45	98.02	71.88	95.37
Right hemisphere	97.09	96.92	50	92	97.99	97.65	62.5	91
Left frontal	93.98	92.65	56.25	86.98	95.08	95.64	68.75	86.02
Left temporal	92.35	92.09	59.38	82.98	97.85	96.97	65.63	84.35
Left occipital	94.75	94.27	62.5	81.07	97.05	97.01	56.25	88.19
Right frontal	96.77	95.98	46.88	84.48	95.77	94.95	62.50	82.83
Right temporal	97.12	96.54	59.38	83.22	99.11	98.88	68.75	85.02
Right occipital	96.98	96	71.88	85.25	97.78	97	59.38	87.41

Table 3. Sensitivity comparison of several classification models

Area	First Experimental Condition				Second Experimental Condition			
	SW-NB	NB	SVM	RF	SW-NB	NB	SVM	RF
Entire brain	97.65	97.64	64.71	96.43	98.64	97.99	88.24	98.73
Left hemisphere	97.03	97	70.59	93.37	99.00	98.67	94.12	97.41
Right hemisphere	96.10	96.02	64.71	90.40	98.11	98	76.14	90.75
Left frontal	95.34	95	64.71	89.12	98.94	98.54	88.24	89.77
Left temporal	90.92	89.66	64.71	81.36	96.92	96.45	82.35	85.27
Left occipital	91.65	89.99	64.71	81.02	94.77	93.76	76.47	90.38
Right frontal	92.65	90.56	52.94	84.85	96.32	95.98	82.24	82.12
Right temporal	91.54	90.65	58.82	81.44	95.99	95.68	76.47	82.91
Right occipital	90.32	90.08	76.47	82.89	95.98	95	76.47	86.88

Table 4. Specificity comparison of several classification models

Area	First Experimental Condition				Second Experimental Condition			
	SW-NB	NB	SVM	RF	SW-NB	NB	SVM	RF
Entire brain	97.54	97.34	53.33	96.1	99.14	98.76	66.67	97.39
Left hemisphere	97.23	97	60	92.58	97.93	94.99	46.67	93.39
Right hemisphere	96.43	96	33.33	94.74	99.03	96	46.67	91.23
Left frontal	96.71	96	46.67	84.49	98.11	98	46.67	82.68
Left temporal	94.53	93.28	53.33	85.19	98.66	98	53.33	86.07
Left occipital	92.87	90.67	53.33	81.14	97.71	97.43	53.33	83.12
Right frontal	93.98	91.76	60	83.87	95.87	95.01	26.67	82.91
Right temporal	91.08	90.56	33.33	85.87	95.08	94.89	53.33	86.88
Right occipital	90.99	90	40	88.84	97.43	94.32	60	89.34

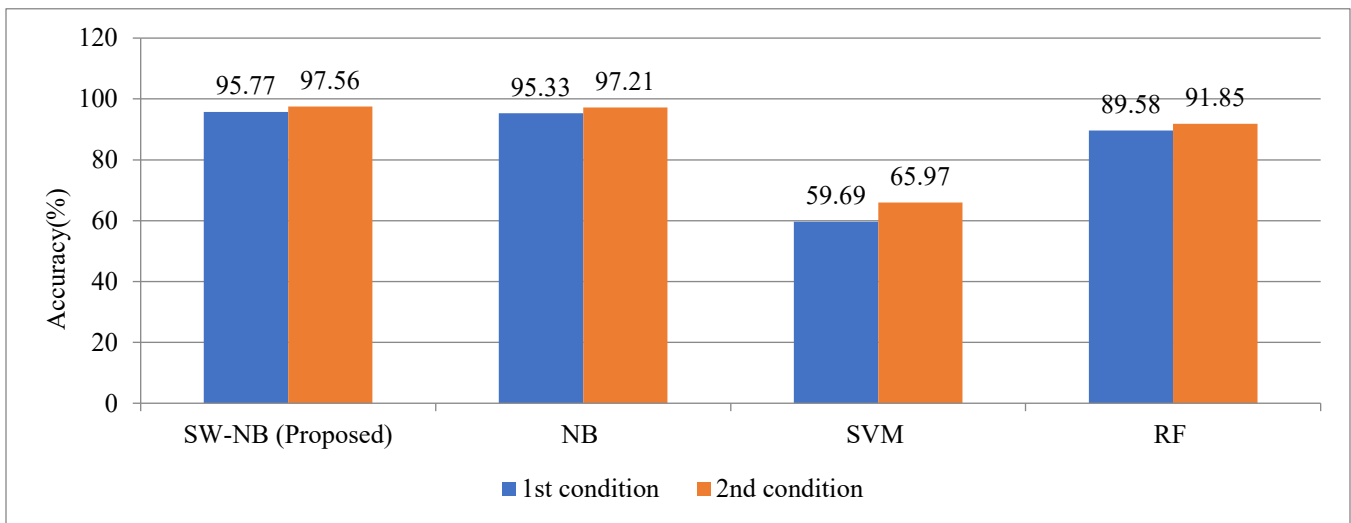


Fig. 5 Accuracy comparison

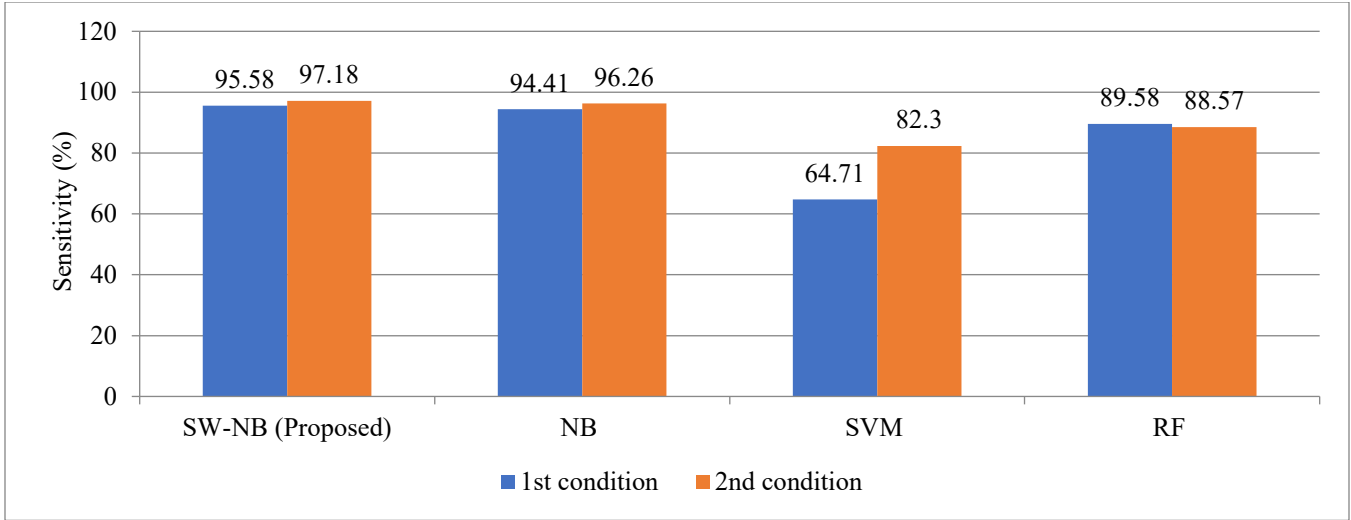


Fig. 6 Sensitivity comparison

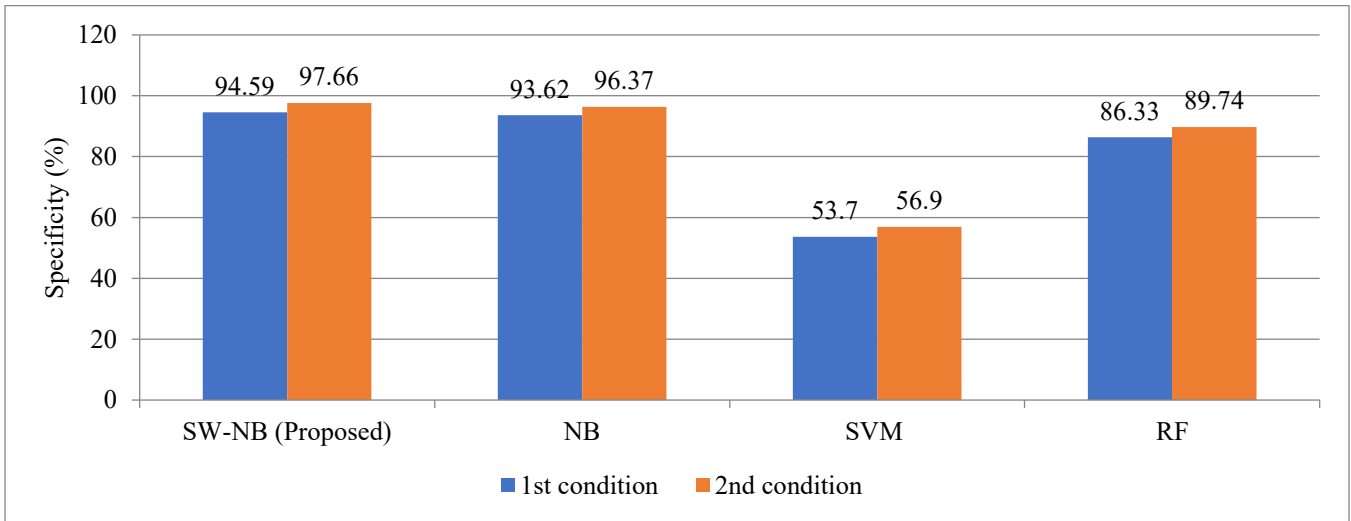


Fig. 7 Specificity comparison

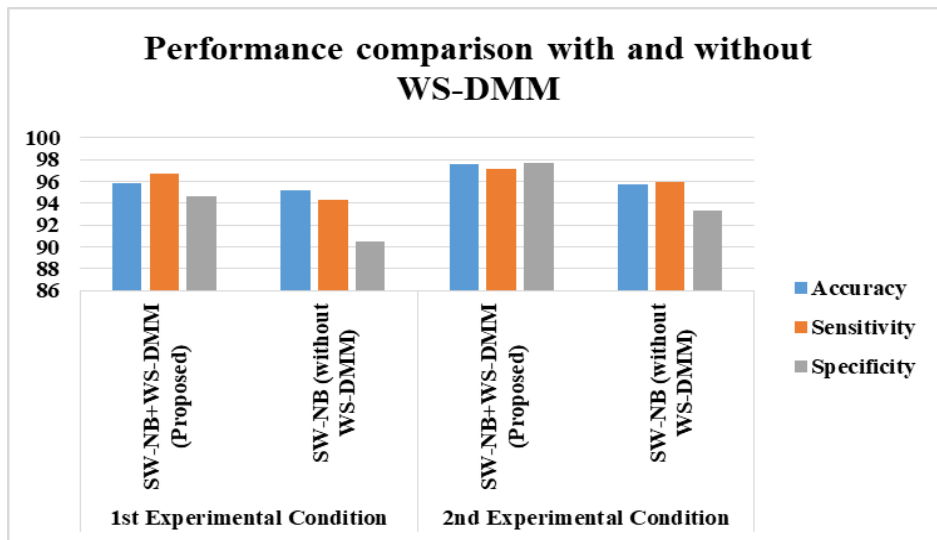


Fig. 8 Performance comparison of the proposed classification model with and without WS-DMM

The mean values of sensitivity, accuracy, and specificity of all compared classifiers are calculated for both experimental conditions, and the graphical comparisons for the calculated average values are offered in Figures 5, 6 and 7, respectively.

Figure 5 shows that the proposed SW-NB classification model attains the maximum accuracy of 97.56% during the second experimental condition and 95.77% during the 1st experimental state. NB classifier attains the 2nd maximum accuracy of 97.21% during the second experimental condition and 95.33% during the first experimental condition. The SVM classifier attains the lowest accuracy of 59.69% during the first experimental condition and 65.97% during the second experimental condition while RF stood intermediate with values of 91.85% during the second experimental condition and 89.58% during the first experimental condition.

Figure 6 shows that the proposed SW-NB classification model attains the maximum sensitivity of 97.18% during the second experimental condition and 95.58% during the first experimental condition. NB classifier attains the second maximum sensitivity of 96.26% during the second experimental condition and 94.41% during the first experimental condition. The SVM classifier attains the least sensitivity of 82.3% during the second experimental condition and 64.71% during the first experimental condition while RF shows moderate performance 88.57% during the second experimental condition and 89.58% during the first experimental condition

Figure 7 shows that the proposed SW-NB classification model attains the maximum specificity of 97.66% during the second experimental condition and 94.59% during the first experimental condition. NB classifier attains the second maximum specificity of 96.37% during the second experimental condition and 93.62% during the first experimental condition. The SVM classifier attains the least

specificity of 56.9% during the second experimental condition and 53.7% during the first experimental condition whereas RF performed at 89.74% during the second experimental condition and 86.33% during the first experimental condition.

The superior performance of the proposed model depends not only on the classifier but also on the WS-DMM model introduced for feature extraction. Figure 8 compares the proposed classification model (SW-NB) with and without WS-DMM. The experimental findings for the second condition demonstrated high accuracy in classifying subjects with and without dyslexia, as differences were observed in the activation of the occipital and parietal regions of both hemispheres when subjects responded to visual stimuli.

5. Conclusion

The goal of the research presented in this paper is to accurately identify dyslexia in kids by analysing their confusing brainwave data. In order to achieve this, we have developed a brand-new WS-DMM model that efficiently classifies people with dyslexia by extracting valuable signal representations. Furthermore, we have combined the benefits of the SW algorithm with the conventional NB classifier to manage the interconnected elements included in the extracted features efficiently. Experiments were conducted under two circumstances, such as audio recognition and visual discrimination, to demonstrate the significance of the suggested classification model. The findings demonstrate that the suggested classification model outperforms the other classifiers in both circumstances. Furthermore, it has been demonstrated that using WS-DMM ensures a notable enhancement in performance. This study contributes valuable insights into the distinct brainwave patterns of dyslexic students, serving as a foundation for future research. Over time, these findings could complement traditional dyslexia diagnosis methods by incorporating neurological aspects, leading to a more comprehensive understanding of the condition.

References

- [1] P. Virtala et al., "Poor Neural and Perceptual Phoneme Discrimination during Acoustic Variation in Dyslexia," *Scientific Report*, vol. 10, no. 1, pp. 1-11, 2020. [[CrossRef](#)] [[Google Scholar](#)] [[Publisher Link](#)]
- [2] P. Tamboer et al., "Machine Learning and Dyslexia: Classification of Individual Structural Neuroimaging Scans of Students with and without Dyslexia," *NeuroImage Clinical*, vol. 11, pp. 508-514, 2016. [[CrossRef](#)] [[Google Scholar](#)] [[Publisher Link](#)]
- [3] Stavros I. Dimitriadis, "Aberrant Resting-State Functional Brain Networks in Dyslexia: Symbolic Mutual Information Analysis of Neuromagnetic Signals," *International Journal of Psychophysiology*, vol. 126, pp. 20-29, 2018. [[CrossRef](#)] [[Google Scholar](#)] [[Publisher Link](#)]
- [4] Janet Giehl, Nima Noury, and Markus Siegel, "Dissociating Harmonic and Non-Harmonic Phase-Amplitude Coupling in the Human Brain," *NeuroImage*, vol. 227, 2021. [[CrossRef](#)] [[Google Scholar](#)] [[Publisher Link](#)]
- [5] Lincoln J. Colling, Hannah L. Noble, and Usha Goswami, "Neural Entrainment and Sensorimotor Synchronization to the Beat in Children with Developmental Dyslexia: An EEG Study," *Frontiers in Neuroscience*, vol. 11, 2017. [[CrossRef](#)] [[Google Scholar](#)] [[Publisher Link](#)]
- [6] Peter Raatikainen et al., "Detection of Developmental Dyslexia with Machine Learning Using Eye Movement Data," *Array*, vol. 12, 2021. [[CrossRef](#)] [[Google Scholar](#)] [[Publisher Link](#)]
- [7] Piotr Plonski et al., "Multi-Parameter Machine Learning Approach to the Neuroanatomical Basis of Developmental Dyslexia," *Human Brain Mapping*, vol. 38, no. 2, pp. 900-908, 2017. [[CrossRef](#)] [[Google Scholar](#)] [[Publisher Link](#)]

- [8] G. Vanitha, and M. Kasthuri, "Performance Analysis of Feature Selection and Classification Methods for Predicting Dyslexia," *Indian Journal of Science and Technology*, vol. 16, no. 33, pp. 2663-2669, 2023. [[CrossRef](#)] [[Google Scholar](#)] [[Publisher Link](#)]
- [9] A. Jothi Prabha, and R. Bhargavi, "Prediction of Dyslexia from Eye Movements Using Machine Learning," *IETE Journal of Research*, vol. 68, no. 2, pp. 814-823, 2022. [[CrossRef](#)] [[Google Scholar](#)] [[Publisher Link](#)]
- [10] Nicolas J. Gallego-Molina et al., "Complex Network Modelling of EEG Band Coupling in Dyslexia: An Exploratory Analysis of Auditory Processing and Diagnosis," *Knowledge-Based Systems*, vol. 240, 2022. [[CrossRef](#)] [[Google Scholar](#)] [[Publisher Link](#)]
- [11] Oded Ghitza, "Acoustic-Driven Delta Rhythms as Prosodic Markers," *Language, Cognition and Neuroscience*, vol. 32, no. 5, pp. 545-561, 2017. [[CrossRef](#)] [[Google Scholar](#)] [[Publisher Link](#)]
- [12] Rosa S. Gisladottir, Sara Bögels, and Stephen C. Levinson, "Oscillatory Brain Responses Reflect Anticipation during Comprehension of Speech Acts in Spoken Dialog," *Frontiers in Human Neuroscience*, vol. 12, 2018. [[CrossRef](#)] [[Google Scholar](#)] [[Publisher Link](#)]
- [13] Usha Goswami, "A Temporal Sampling Framework for Developmental Dyslexia," *Trends in Cognitive Sciences*, vol. 15, no. 1, pp. 3-10, 2010. [[CrossRef](#)] [[Google Scholar](#)] [[Publisher Link](#)]
- [14] Ihsan Ullah et al., "An Automated System for Epilepsy Detection Using EEG Brain Signals Based on Deep Learning Approach," *Expert Systems with Applications*, vol. 107, pp. 61-71, 2018. [[CrossRef](#)] [[Google Scholar](#)] [[Publisher Link](#)]
- [15] Rabindra Gandhi Thangarajoo et al., "Machine Learning-Based Epileptic Seizure Detection Methods Using Wavelet and EMD-Based Decomposition Techniques: A Review," *Sensors*, vol. 21, no. 24, pp. 1-34, 2021. [[CrossRef](#)] [[Google Scholar](#)] [[Publisher Link](#)]
- [16] Samanwoy Ghosh-Dastidar, Hojjat Adeli, and Nahid Dadmehr, "Mixed-Band Wavelet-Chaos-Neural Network Methodology for Epilepsy and Epileptic Seizure Detection," *IEEE Transactions on Biomedical Engineering*, vol. 54, no. 9, pp. 1545-1551, 2007. [[CrossRef](#)] [[Google Scholar](#)] [[Publisher Link](#)]
- [17] Alexandros T. Tzallas, Markos G. Tsipouras, and Dimitrios I. Fotiadis, "Epileptic Seizure Detection in EEGs Using Time-Frequency Analysis," *IEEE Transactions on Information Technology in Biomedicine*, vol. 13, no. 5, pp. 703-710, 2009. [[CrossRef](#)] [[Google Scholar](#)] [[Publisher Link](#)]
- [18] Y.U. Khan, and J. Gotman, "Wavelet Based Automatic Seizure Detection in Intracerebral Electroencephalogram," *Clinical Neurophysiology*, vol. 114, no. 5, pp. 898-908, 2003. [[CrossRef](#)] [[Google Scholar](#)] [[Publisher Link](#)]
- [19] Mingyang Li, Wanzhong Chen, and Tao Zhang, "Automatic Epilepsy Detection Using Wavelet-Based Nonlinear Analysis and Optimized SVM," *Biocybernetics and Biomedical Engineering*, vol. 36, no. 4, pp. 708-718, 2016. [[CrossRef](#)] [[Google Scholar](#)] [[Publisher Link](#)]
- [20] Diego Castillo-Barnes et al., "Probabilistic and Explainable Modeling of Phase-Phase Cross-Frequency Coupling Patterns in EEG, Application to Dyslexia Diagnosis," *Biocybernetics and Biomedical Engineering*, vol. 44, no. 4, pp. 814-823, 2024. [[CrossRef](#)] [[Google Scholar](#)] [[Publisher Link](#)]
- [21] Shankar Parmar, and Chirag Paunwala, "A Novel and Efficient Wavelet Scattering Transform Approach for Primitive-Stage Dyslexia-Detection Using Electroencephalogram Signals," *Healthcare Analytics*, vol. 3, 2023. [[CrossRef](#)] [[Google Scholar](#)] [[Publisher Link](#)]
- [22] Guhan Seshadri N.P., "EEG Based Classification of Children with Learning Disabilities Using Shallow and Deep Neural Network," *Biomedical Signal Processing and Control*, vol. 82, 2023. [[CrossRef](#)] [[Google Scholar](#)] [[Publisher Link](#)]
- [23] Nicolás J. Gallego-Molina et al., "Unraveling Brain Synchronisation Dynamics by Explainable Neural Networks Using EEG Signals: Application to Dyslexia Diagnosis," *Interdisciplinary Sciences: Computational Life Sciences*, vol. 16, pp. 1005-1018, 2014. [[CrossRef](#)] [[Google Scholar](#)] [[Publisher Link](#)]
- [24] Zbigniew Gomolka et al., "Diagnosing Dyslexia in Early School-Aged Children Using the LSTM Network and Eye Tracking Technology," *Applied Sciences*, vol. 14, no. 17, pp. 1-24, 2024. [[CrossRef](#)] [[Google Scholar](#)] [[Publisher Link](#)]
- [25] Radford M. Neal, "Markov Chain Sampling Methods for Dirichlet Process Mixture Models," *Journal of Computational and Graphical Statistics*, vol. 9, no. 2, pp. 249-265, 2000. [[CrossRef](#)] [[Google Scholar](#)] [[Publisher Link](#)]
- [26] Milena Cukic et al., "The Successful Discrimination of Depression from EEG Could be Attributed to Proper Feature Extraction and not to a Particular Classification Method," *Cognitive Neurodynamics*, vol. 14, pp. 443-455, 2020. [[CrossRef](#)] [[Google Scholar](#)] [[Publisher Link](#)]
- [27] Harshani Perera et al., "EEG Signal Analysis of Writing and Typing between Adults with Dyslexia and Normal Controls," *International Journal of Interactive Multimedia and Artificial Intelligence*, vol. 5, no. 1, pp. 62-67, 2018. [[CrossRef](#)] [[Google Scholar](#)] [[Publisher Link](#)]
- [28] Pavlos Christodoulides et al., "Classification of EEG Signals from Young Adults with Dyslexia Combining a Brain Computer Interface Device and an Interactive Linguistic Software Tool," *Biomedical Signal Processing and Control*, vol. 76, 2022. [[CrossRef](#)] [[Google Scholar](#)] [[Publisher Link](#)]